CI&CEQ
Chemical Industry & Chemical Engineering Quarterly

Available online at
Association of the Chemical Engineers of Serbia AChE
www.ache.org.rs/CICEQ

Chem. Ind. Chem. Eng. Q. 31 (1) 23–31 (2025) CI&CEQ

SURESHKUMAR PETCHIMUTHU[1]

SATHIYA MOORTHY RAJENDRAN[2]

[1]Department of Mechanical Engineering, Government College of Engineering, Tirunelveli, India

[2]Department of Mechanical Engineering, Anna University Regional Campus, Coimbatore, India

EXPERIMENTAL STUDY OF SOLAR AIR HEATER WITH C-SHAPED RIBS COATED WITH ZEOLITE

Article Highlights

- Improve the performance of an SAH using C-ribs with zeolite coating on the absorber plate
- A high rib height promotes increased turbulence and mixing of air flowing through the SAH duct
- Smaller holes can exaggerate heat transfer and enhance the cross-flow effect
- Zeolite coatings, serve to enhance the thermal performance by desorption and adsorption processes

Abstract

A study was conducted to determine the heat transmission rate and friction properties of a solar air heater's (SAH) absorber by including a c-shaped rib, with and without perforations, and the efficiency of this absorber with and without zeolite coating was investigated. This research is carried out by varying Reynolds numbers (Re) ranges between 3000 to 18000, the height of the C-shaped rib (e) ranges between 2 mm to 4 mm, and the embedded hole diameter in the C-shaped rib ranges between 1 mm to 3 mm. The impact of rib height, hole diameter, and zeolite coating on thermal efficiency and Nusselt number is compared to a flat channel under the same flow environments. A strong secondary flow is created by the free shear layer reattaching more often at higher rib heights, and a smaller hole can exaggerate heat transfer and enhance the cross-flow effect. The thermal efficiency and Nusselt number of the solar air heater with c-ribs (Rib height = 4 mm and hole diameter = 1 mm) and zeolite coating on the absorber increased by 29.7% and 62.2% over the flat absorber. Ribs 4 mm high can increase duct friction by up to 3.1 times compared to a smooth duct.

Keywords: C-shaped ribs; perforations; zeolite coating; thermal performance; friction factor.

SCIENTIFIC PAPER

UDC 66.024.1:536:549.67

Solar air heaters are a fundamental part of solar energy utilization systems. They are designed to absorb incoming solar light and convert it into thermal energy at the absorber plate. The heated absorber plate transfers thermal energy to the air passing through the duct via convection. The thermal energy stored in the hot absorber plate is transferred to the air because of the temperature disparity. This process heats the air as it passes through the SAH. These SAH systems are used in various applications for heating purposes, including space heating, preheating air for combustion processes, drying crops, desalination (evaporating seawater to produce fresh water), and water heating. The efficiency of flat SAHs is low because there is not enough convective heat transfer between the fluid and the absorber. Consequently, the temperature of the absorber rises, and more heat emission to the atmosphere is higher. The existence of a viscous sub-layer is most often due to poor heat transfer; this layer can be eliminated by roughening the absorber. Various techniques, including the incorporation of fins, artificial roughness, and packed beds within ducts, have been proposed as methods to enhance thermal performance. Implementing

Correspondence: S. Petchimuthu, Department of Mechanical Engineering, Government College of Engineering, Tirunelveli 627007, India.
E-mail: ppskumar200@gmail.com
Paper received: 30 December, 2023
Paper revised: 11 March, 2024
Paper accepted: 27 March, 2024

https://doi.org/10.2298/CICEQ231230010P

roughened surfaces on the absorber plate, such as ribbed or corrugated surfaces, disrupts laminar airflow and promotes turbulence. This improves the transfer of heat from the absorber to the air. Applying selective coatings to the absorber plate maximizes solar absorption while minimizing thermal radiation losses, improving overall efficiency.

Yadav *et al*. [1] tested the impact of a circular rib positioned in an angular arc approach and discovered that heat transmission and friction were greater than the flat one. Lanjewar *et al*. [2], investigating the influence of W-shaped ribs as an artificial element, found that thermo-hydraulic performance was extreme at a slant of attack of 60°. Pandey *et al*. [3] explored the impact of relative roughness height, arc angle, pitch, width, and gap distance on Nusselt number (Nu), and friction (*f*) using multiple-arc-shaped ribs fixed over an absorber. The author found that Nu = 5.85 and *f* = 4.96 were superior to flat channels. Saini *et al*. [4] probed the impact of ribs with dimple forms over the Nusselt number and friction factor. Unlike flat absorbers, ribs considerably improved Nu and friction qualities. Varun *et al*. [5] researched the impact of inclined and transverse ribs above the absorber. At a relative roughness pitch of 8, a higher thermal efficiency was reached. Kumar *et al*. [6] experimented with the impact of separate W-shaped ribs and discovered that the Nusselt number and friction factor of 1.67 and 1.82, respectively, were attained at an angle of attack of 60°. Sahu and Prasad [7] theoretically investigated arc-shaped wire protrusions over the absorber. They reported that the roughness height of 0.0422 improved the exergetic efficiency by 56% compared to the flat absorber.

Jin *et al*. [8] numerically analyzed the impact of an artificial roughness of many V-shaped ribs over the absorber. They stated that V-shaped ribs create streamwise helical vortex flows that augment the performance of SAHs. Yadav and Bhagoria [9] revealed by a numerical study that square-separated transverse rib along relative roughness, pitch, and height gave a better thermo-hydraulic performance.

Aharwal *et al*. [10] researched the impact of gap width and the position of a slanted continuous rib on heat transfer and the friction factor. The optimal width of 1.0 and the position of 0.25 provided better thermo hydraulic performance. Sahu and Bhagoria [11] explored the effect of the heat transmission coefficient in 90°-broken ribs and found that the thermal efficiency ranged from 51% to 83.5%. Hans *et al*. [12] studied the outcome of several V-ribs on the absorber of a SAH in the following ranges: Re from 2000 to 20000, *e*/*D* from 0.019 to 0.043, *P*/*e* from 6 to12, a from 30° to 75°, and *W*/*w* from 1 to 10. They found that the heat transfer and friction were six- and five-fold greater compared with the flat absorber. Ghritlahre *et al*. [13] examined the thermal performance and heat transfer of an arc-shaped roughened SAH with two different airflow orientations: apex up and apex down. The experiments were conducted using different mass flow rates, spanning from 0.007 kg/s to 0.022 kg/s. The roughness parameters taken into study included “relative roughness pitch, relative roughness height, rib roughness, and arc angle”. The heat transfer in the apex-up configuration was 33.2% more efficient than the apex-down arrangement. These results suggest that the rib roughness absorber with the apex-up airflow with wire is more efficient than the apex down airflow of the SAH.

Agrawal *et al*. [14] empirically studied the impact of double arc reverse formed along a consistent gap and discovered a Nusselt number of 2.85 and a friction factor of 2.42, both of which were higher than those of a flat absorber. Singh *et al*. [15] examined the effect of several arc ribs on thermal performance. They discovered a huge increment of Nusselt number (5.07) and friction factor (3.71) compared to the flat one.

Kumar *et al*. [16] experimentally researched the impact of nanomaterial interfering with a black-paint covering on an absorber. They concluded that the entropy formation rises with increasing the flow rate. Exergy effectiveness for BP-2 was 4.27% greater than that for BP-1. Jelonek *et al*. [17] studied the effectiveness of a new sand-plastered and sand-packed (SCSF) polycarbonate sheet of a solar air collector (SAC). It was discovered that the SAC with storing offered 39% and 20% greater efficiency than the other two. After an extensive survey, it could be inferred that researchers have worked on varying the geometric parameters like Rib roughness, height, pitch, and coating over the absorber for better thermal performance of SAHs.

In light of the foregoing, the present study was conducted to determine Nusselt number and friction characteristics over the heated surface using a C-shaped rib with and without holes embedded in it to generate vortices as a roughness element on the absorber surface. The C-shaped rib configuration can induce strong vortices and turbulence in the boundary layer flow. This enhanced turbulence promotes better mixing and heat transfer amid the fluid and the solid surface, leading to improved convective heat transfer coefficients. Compared to other rib configurations, such as rectangular or trapezoidal ribs, the C-shaped rib may offer the advantage of a lower pressure drop. The streamlined shape of the C rib could help minimize flow resistance while still effectively enhancing heat transfer. The experiment was also carried out by adding

a zeolite coating to the absorber plate. Researchers have looked at a wide variety of roughness element forms and sizes, but none have made an effort to test the effects of the current geometry and coating on heat convection.

MATERIAL AND METHODS

Materials

The effects of several C-shaped ribs on heat transfer and frictional properties of SAH have been studied in the experiment. Fig. 1 provides a graphical depiction of the experiment. The air duct is split into three distinct areas: entrance, testing, and exit. The entire duct is 1750 mm long, with a testing section length of 1000 mm having a corresponding 80 mm hydraulic diameter. The lengths of the entering and exiting segments are 500 mm and 250 mm, respectively. To determine proper entry and exit dimensions, ASHRAE standard 93-77 was used as a reference. According to it, the minimum inlet and outlet lengths for the zig-zag flow regime should be $5\sqrt{WH}$ and $2.5\sqrt{WH}$, respectively. Improved airflow across the absorber's surface was achieved by inserting guide vanes at the inlet. Wood was chosen as the duct's primary construction material because it was affordable, abundant, and good at insulating. A GI sheet absorber plate of 3 mm thickness was made. The upper surface of the absorber was artificially roughened using riveted C-shaped ribs. The absorber plate was made as the duct bottom wall, and the glass wool was used to insulate the sidewalls.

To measure the input and output air temperatures, thermocouples have been installed. Calibrated K-type thermocouples with digital displays, showing output in degrees Celsius with an accuracy of 0.1 °C, were employed to determine the air and absorber plate temperatures across multiple locations. A standard thermometer was used to calibrate the thermocouples. The position of the twelve thermocouples installed at regular intervals to gauge the average temperature of the absorber is shown in Fig. 2a. A calibrated orifice meter coupled with a U-tube manometer was included for determining the airflow rate. A Pitot tube was utilized for the orifice plate calibration. The inlet flow rate was regulated by a regulating valve at the entry. The pressure downfall in the test area was measured with a digital micromanometer. Rib placements above the absorber are shown in Fig. 2b.

Methods

Before the commencement of the experiment, the parts and instruments were tested for functionality. Under steady-state conditions, the requisite heat

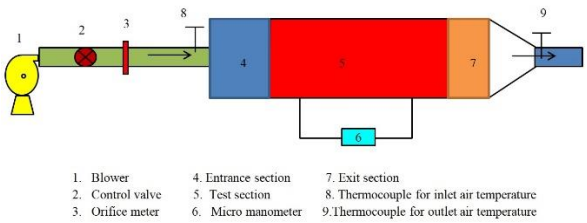

Figure 1. The experiment setup.

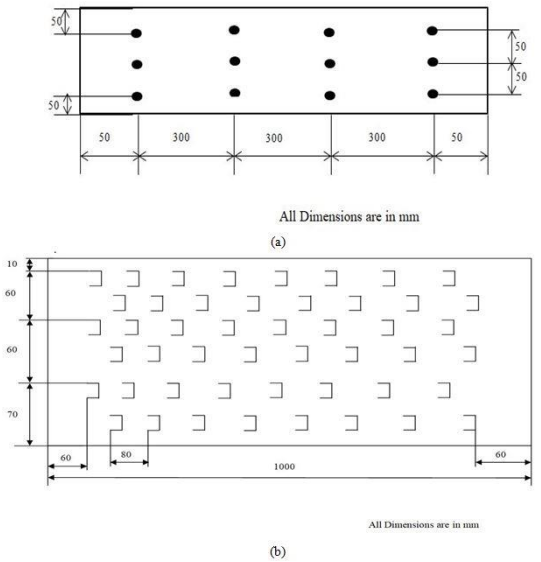

Figure 2. (a) Thermocouples fixed over the test section; (b) Rib positions over the absorber plate.

transfer investigations were carried out. The airflow rate ranged between 0.0064 kg/s and 0.0386 kg/s with four in-between values to represent all possible variations of the Reynolds number from 3,000 to 18,000 respectively.

The average solar intensity (I) was 800 W/m^2 at Bodinayakanur, Tamil Nadu, India, in May 2023. Since the working fluid was air, density, specific heat, thermal conductivity, and dynamic viscosity are 1.225 kg/m^3, 1006 J/kg K, 0.0262 W/m K, 1.81×10^{-5} kg/m s, respectively.

The following variables were assessed during experimentation: air temperature at entry, air temperature at exit, mean temperature of the absorber plate, pressure drop across the test section.

Data reduction

The airflow rate, the heat transfer to the air, the Nusselt number, the heat transfer coefficient, and the friction factor were quantified with available data from the present study.

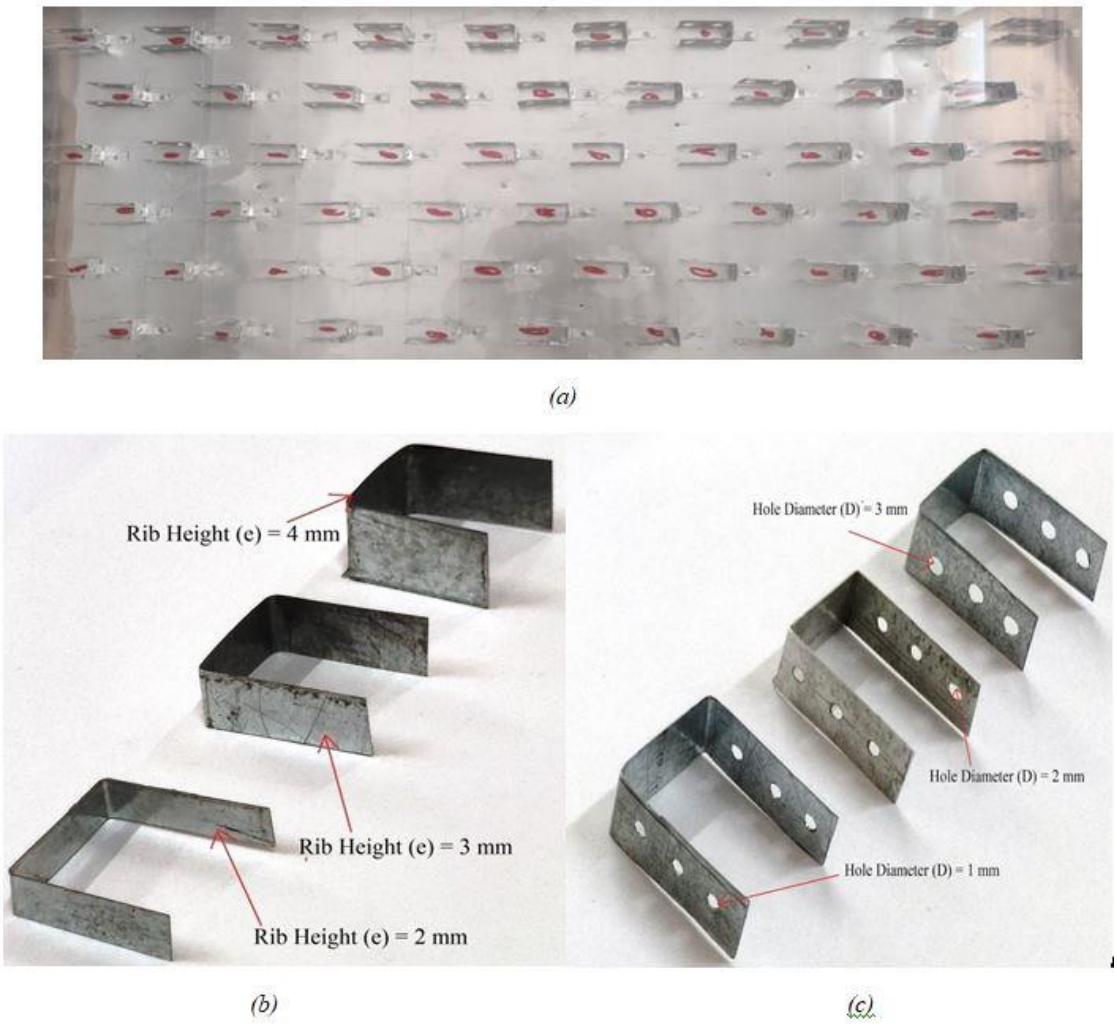

Figure 3. (a) Pictorial view of e = 4 mm, D = 1 mm and zeolite coating; (b) Enlarged view of rib heights; (c) Enlarged view of a rib height (e) = 4 mm and hole diameters of 1, 2 and 3 mm.

The necessary parameters: the mass flow rate, heat transfer, thermal efficiency, and heat transfer coefficient were evaluated as per the highlighted references deceased [18] using Eqs. (1–4), respectively:

$$m = \rho A V \tag{1}$$

$$Q = mC_p\left(T_0 - T_i\right) \tag{2}$$

$$\eta = \frac{Q}{IA_c} \tag{3}$$

$$h = \frac{Q}{A_c\left(T_p - T_f\right)} \tag{4}$$

where $A = \frac{\pi}{4}d^2$, $T_f = \frac{(T_i+T_o)}{2}$,

$T_p = \frac{(T_1+T_2+T_3+T_4+T_5+T_6+T_7+T_8+T_9+T_{10}+T_{11}+T_{12})}{12}$, and A_c is the length of the absorber × width of the absorber.

The Nusselt number and friction factor for the roughened absorber are defined by Eqs. (5) and (6), respectively:

$$Nu = \frac{hD_h}{k} \tag{5}$$

$$f = \frac{D_h \Delta P}{2LV^2\rho} \tag{6}$$

Validity test

The experimentally obtained Nusselt number and friction factor values in the flat were compared with the value computed by the Dittus-Boelter and Modified Blasius equations, i.e., Eqs. (7) and (8), respectively.

$$Nu_s = 0.023\mathrm{Re}^{0.8}\,\mathrm{Pr}^{0.4} \tag{7}$$

$$f_s = 0.085\mathrm{Re}^{-0.25} \tag{8}$$

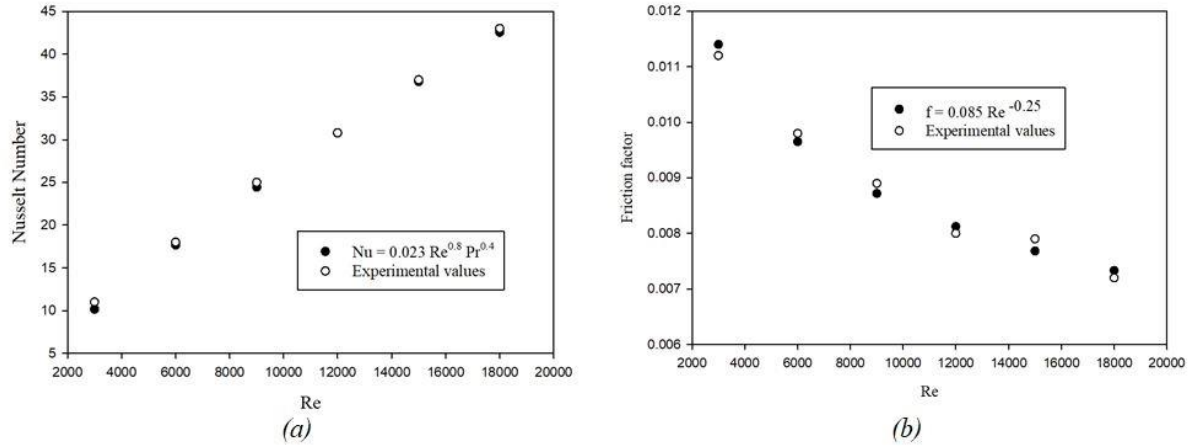

Figure 4. (a) Validation of smooth plate for Nu; (b)Validation of smooth plate for f.

Figs. 4a and 4b graphically represent the experimental and mathematically established Nu and *f*-values, respectively. The mean deviation of Nu and friction factor values were 2.7% and 2.6%, respectively, confirming a high conformity degree between the predicted and the experimental values and thus, validating the setup of the experiment.

Uncertainty analysis

The uncertainty analysis is a useful and efficient tool for developing and planning experiments. Eq. (9) is used to determine the uncertainty measurement:

$$W_R = \sqrt{\left[\left(\frac{\partial R}{\partial x_1} w_1\right)^2 + \left(\frac{\partial R}{\partial x_2} w_2\right)^2 + \ldots\ldots\ldots\ldots + \left(\frac{\partial R}{\partial x_n} w_n\right)^2\right]} \quad (9)$$

where, X_1, X_2 … X_n are the independent variables, and W_1, W_2 … W_n are the uncertainties of the independent variables

Thermal efficiency, Nu, and friction factor uncertainties are 3.20%, 3.32%, and 3.26%, respectively, which are within acceptable ranges. The following uncertainties are associated with the measurements of the mass flow rate, temperature, radiation, pressure drop, duct height, and absorber plate length are ± 0.001 m³/hr, ± 0.1 °C, ± 1 W/m², ± 0.098 Pa, ± 0.1 mm, and ± 0.6 mm, respectively.

RESULTS AND DISCUSSION

The significance of the rib height, hole diameter, and zeolite coating for the heat transmission and friction qualities of a roughened absorber were investigated.

Heat transfer properties

This part of the study focused on examining the thermal characteristics and performance of the SAH system, aiming to a detailed analysis of the heat transfer processes occurred and their impact on the overall system efficiency.

Effect of Reynolds number

As the Reynolds number goes up, the Nusselt number consistently rises because the viscous layer near the surface gets thinner, allowing for more heat transfer. On the other hand, the friction factor consistently falls with increasing the Reynolds number. In smooth ducts with fully developed flow, this decrease is due to less resistance from the thinned viscous sublayer. However, it also means a larger pressure drop along the duct, requiring more pumping power. Adding roughness to the absorber plate disrupts the smooth flow, creating more turbulence and causing a higher friction factor compared to a smooth plate.

Effect of rib height

The effect of rib height (*e*) on the thermal efficiency and Nusselt number for 3,000 < Re < 18,000 is depicted in Figs. 5a and 5b. The thermal efficiency of the SAH is directly proportional to the flow rate at the entry. As the mass flow rate rises, the thermal efficiency increases because more heat is removed by the working fluid. As the rib height increases, the Nusselt number and thermal efficiency increase due to a secondary flow created by the free shear layer at a higher rib height. A high rib height promotes increased turbulence and mixing of air passing through the SAH duct. Turbulence enhances heat transfer by disrupting laminar flow and promoting convective heat exchange between the hot absorber plate and the air. Taller ribs provide a larger surface area for the heat transfer between the absorber and the airflow. This increased surface area allows for greater contact between the

heated absorber and the air, facilitating more efficient heat transfer. In contrast, a low rib height may result in less turbulence and mixing, leading to reduced heat transfer enhancement compared to higher rib heights. Shorter ribs offer less surface area for heat transfer, potentially limiting the effectiveness of convective heat exchange within the SAH duct. Lower rib heights typically result in lower pressure drop and energy losses than higher rib heights. However, the lower rib height reduces the heat transfer efficiency. In addition, by including a C-shaped rib, the local wall turbulence is induced in the heat transmission region. The thermal resistance falls significantly as the heat transfer improves. The main flow impinges on the surface as the rib height increases, increasing the heat transfer rate for all Re values. A reduction in heat transfer from the surface of the absorber is observed if the rib height is beyond 4 mm because the free shear layer cannot rejoin. The reduced rib height allows reconnected air to travel further before colliding with subsequent ribs, enabling the regrowth of a viscous sub-layer on a localized region of the heater's surface. The regrowth of the boundary layer causes a decrease in the Nu number, causing an adverse effect on the heat transfer from the absorber.

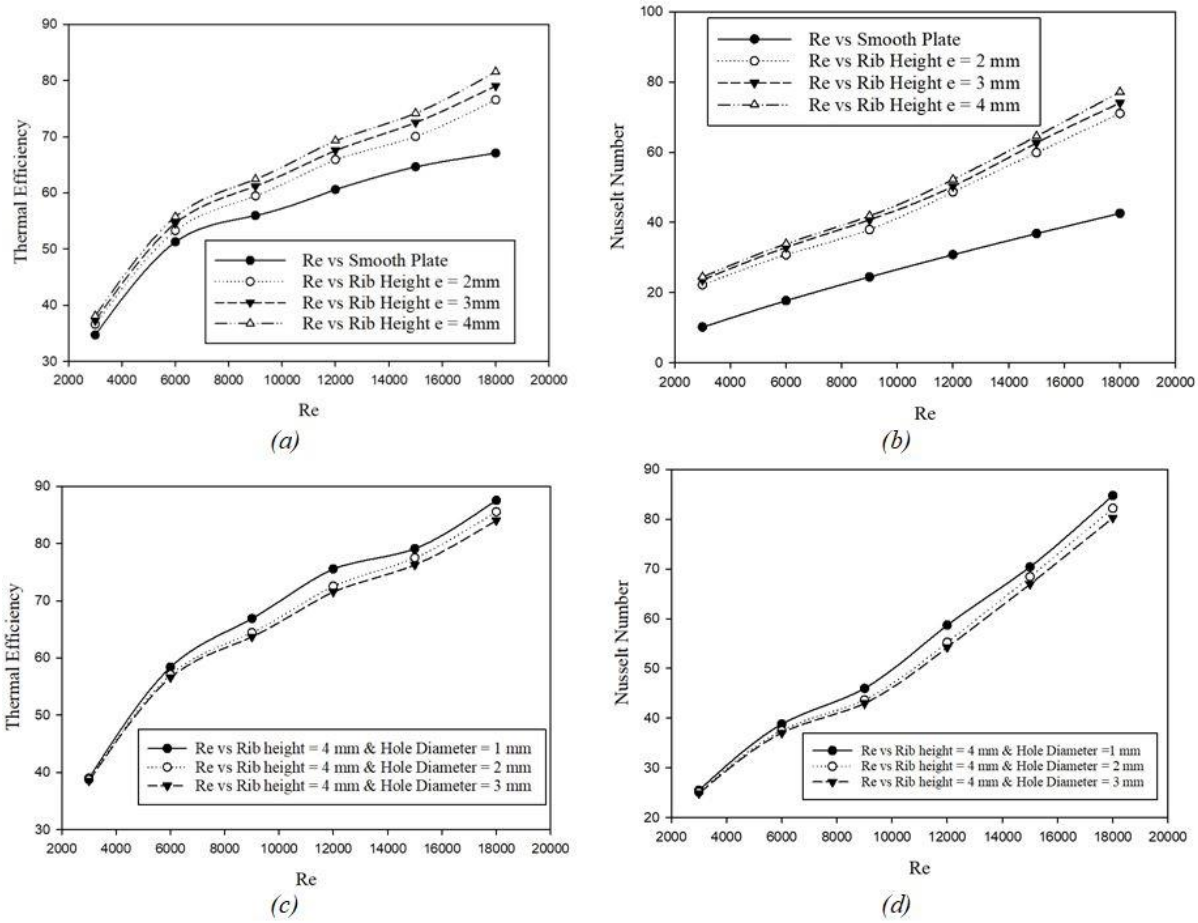

Figure 5. (a) Thermal efficiency vs Re for rib height; (b) Nu vs Re for rib height; (c) Thermal efficiency vs Re for hole diameter; (d) Nu vs Re for hole diameter.

Effect of hole diameter

Figs. 5c and 5d show how the thermal efficiency and Nusselt number are changed as a consequence of the hole diameter for the Re number range applied. As the hole diameter increases, thermal efficiency decreases. A smaller opening can increase the cross-flow effect and heat transfer rate. The C-shaped configuration with a 1 mm hole diameter has the highest exit temperature because the air has to go through a smaller hole before it moves out, so it stays in the test part for a longer duration. Additionally, it generates several small vortices in the rib region, which in turn increases the turbulence responsible for better thermal efficiency and higher Nusselt number. In addition, smaller hole diameters provide a larger surface area for heat transfer between the absorber and the airflow, which facilitates a more effective convective heat exchange and enhances the heat transfer efficiency within the SAH duct. Larger holes do not contribute to enhanced heat transmission because of the sluggish flow regime, and higher hole diameters offer less surface area for heat transfer, potentially limiting the

convective heat exchange and reducing the heat transfer efficiency compared to the systems with smaller hole diameters.

Effect of zeolite coating

Figs. 6a and 6b illustrate the variation in the thermal efficiency and Nusselt number of the zeolite-coated absorber for different Re number values. The rib height of 4 mm and the embedded hole diameter of 1 mm with a zeolite coating enable a better heat transfer rate. Desorption and adsorption techniques are used by the zeolite for storing and releasing heat. In the context of heat storage, adsorption refers to the process where molecules of a gas or vapor adhere to the surface of the zeolite. When a zeolite material is exposed to heat, it can adsorb molecules of a specific gas or vapor, typically water vapor or other volatile organic compounds, into its porous structure. This adsorption process is exothermic, meaning it releases heat energy as the molecules are attracted to the surface of the zeolite. Desorption is the reverse process of adsorption. When the zeolite material is subjected to a decrease in temperature or a decrease in pressure, the adsorbed molecules are released from the surface of the zeolite. This desorption process is endothermic, meaning it requires energy input to break the bonds between the molecules and the zeolite surface. The energy required for desorption is typically supplied in the form of heat, which can be provided by solar energy in solarly air-heated systems. Zeolite naturally has an exothermic characteristic, making it an excellent solar collector for use in thermal applications. Zeolite has around 20% to 50% intra-crystalline voids.

A zeolite coating over the absorber collects the heat from sunlight. Wet air is passed via the air heater to extract and utilize the heat stored in the zeolite-coated absorber. This enables the zeolites to dry the air by adsorbing the water from it. The air warms up as a result of the exothermic adsorption. A strong secondary flow is created by the free shear layer reattaching more often at higher rib heights, and a smaller hole can exaggerate heat transfer and enhance the cross-flow effect. Larger holes do not participate in the enhancement of heat transmission due to the stagnant flow regime. The heat transmission is improved as a result of the smaller holes.

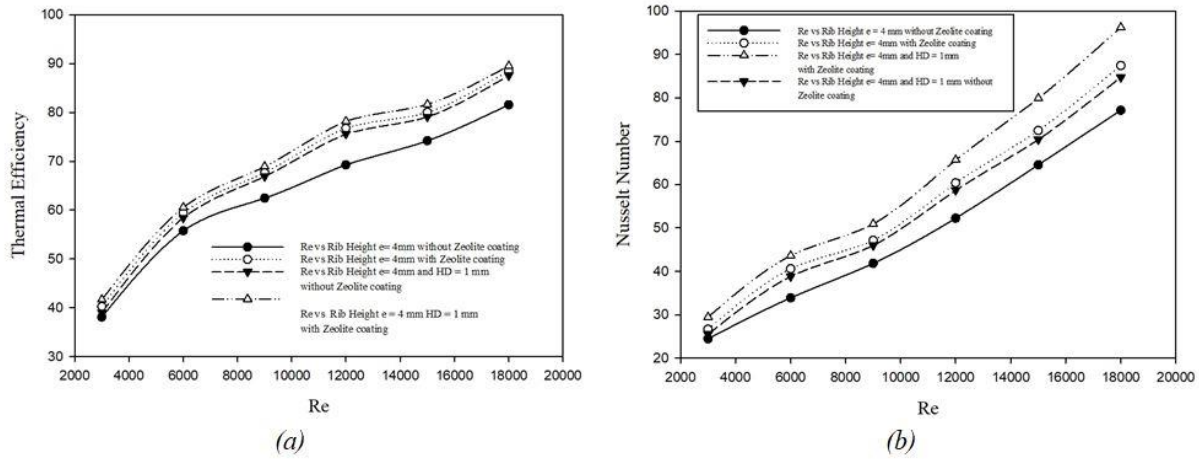

Figure 6. (a)Thermal efficiency vs Re for zeolite coating; (b) Nu vs Re for zeolite coating.

Friction factor characteristics

Fig. 7 shows the impact of hole diameter and rib height on the friction factor for 3000 < Re > 18000. Blasius correlation is used in computing the friction factor for a flat passage. It manifests that the friction factors drop with a rise in the Re number due to the thinning of the viscous sublayer; the Re number increases due to a rise in the mean flow velocity when the friction factor decreases.

As the Re number increases, the pressure in the test region decreases. The friction factor varies inversely to the mean square of the fluid velocity and is directly related to the pressure. Consequently, a rise in the mean fluid velocity predominates over a rise in the pressure downfall. The friction factor declines in tandem with increasing the Re number. The friction factor is larger with the 4 mm rib height compared to that with an embedded hole. As the roughness height rises, so does the friction factor. As rib height increases, the flow becomes more turbulent, causing an increase in the viscous drag over the absorber and ultimately the friction factor rises. Rise in turbulence is not very incisive at lesser rib heights. The holes in the ribs cause an increase in the ratio of the open regions. The higher the ratio of the open region, the lower the pressure within the SAH, as the friction factor is significantly reduced due to a decrease in pressure loss compared to ribs without perforations.

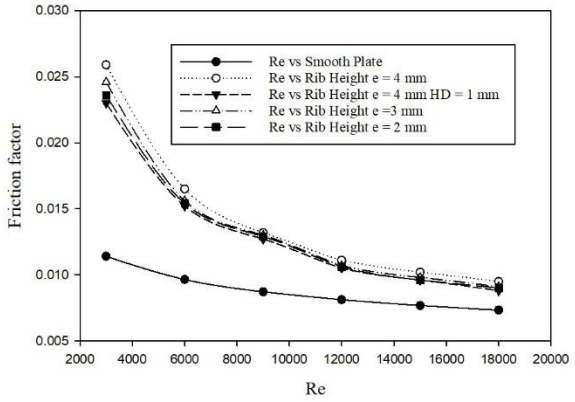

Figure 7. Friction factor vs Re.

Comparison of C-shaped, V-shaped, and circular ribs

Compared to V-shaped and circular ribs, C-ribs offer potentially superior heat transfer due to their open face facilitating better air contact with the collector plate and more efficient heat transfer from the absorber to the air. Additionally, C-shaped ribs might have a lower pressure drop because of the larger flow passage area they create. On the other hand, V-shaped and circular ribs generally have moderate heat transfer and pressure drop characteristics. These are used for space heating in winter sessions. C-shaped ribs can enhance heat transfer, potentially allowing for a smaller collector size to meet heating needs, which can be beneficial for space-constrained rooftops.

CONCLUSION

These inferences can be made based on the findings of this experimental study. As the Re number increases, the thermal performance rises and the friction falls. The friction and thermal properties of a C-rib are higher when compared to a flat absorber. This is because roughness changes the flow properties, leading to flow separation, the creation of secondary flows, and reattachments.The thermal efficiency and Nu number of the SAH with C-ribs (rib height = 4 mm and hole diameter = 1 mm) and the zeolite coating on the absorber increased by 29.7% and 62.2%, respectively, over the flat absorber. A strong secondary flow is created by the free shear layer reattaching more often at higher rib heights, and a smaller hole can exaggerate heat transfer and enhance the cross-flow effect. Desorption and adsorption techniques are used by the zeolite for storing and releasing heat due to the inherent exothermic property of zeolite, which makes it suitable for efficiently harvesting solar energy for heating applications. 4 mm high ribs can increase duct friction by up to 3.1 times compared to a smooth duct. In the presence of roughness, the flow becomes more turbulent, causing an increase in the viscous drag over the absorber compared to the smooth configuration.

NOMENCLATURE

A_c	Area of collector plate (m^2)
C_p	Specific heat of air at constant pressure (J/kgK)
D	Hole diameter (mm)
D_h	Hydraulic diameter (mm)
f	Friction factor
I	Incident radiation (W/m^2)
m	Mass flow rate(kg/s)
Nu	Nusselt number
p	longitudinal pitch
P	Pressure (Pa)
Pr	Prandtlnumber
q	Heat gain (W)
Re	Reynolds number
T_i	Temperature at the entrance (K)
T_o	Temperature at the exit (K)
ΔT	Difference in temperature (K)
v	Mean flow velocity (m/s)
Greek symbols	
ρ	Specific mass (kg/m^3)
μ	Absolute viscosity of the working fluid (kg/m s)
η	Thermal efficiency
Subscripts	
h	hydraulic
i	inlet
o	outlet
p	plate
Abbreviations	
SAC	Solar air collector
SAH	Solar air heater
SCSF	Sand coated and sand filled

REFERENCES

[1] S. Yadav, M.Kaushal, Varun, Siddhartha, Exp. Therm. Fluid Sci. 44 (2013) 34–41. https://doi.org/10.1016/j.expthermflusci.2012.05.011.

[2] A. Lanjewar, J.L. Bhagoria, R. Sarviya, Exp. Therm. Fluid Sci. 35 (6) (2011) 986–995. https://doi.org/10.1016/j.expthermflusci.2011.01.019.

[3] N. K. Pandey, V.K. Bajpai, Varun, Sol. Energy 134 (2016) 314–326. https://doi.org/10.1016/j.solener.2016.05.007.

[4] R.P. Saini, J. Verma, Energy 33 (8) (2008) 1277–1287. https://doi.org/10.1016/j.energy.2008.02.017.

[5] Varun, R.P. Saini, S.K. Singal, Renewable Energy 33 (6) (2008) 1398–1405. https://doi.org/10.1016/j.renene.2007.07.013.

[6] A. Kumar, J.L. Bhagoria, R.M. Sarviya, Energy Convers. Manage. 50 (8) (2009) 2106–2117. https://doi.org/10.1016/j.enconman.2009.01.025.

[7] M.K. Sahu, R.K. Prasad, Renewable Energy 96 (2016) 233–243. https://doi.org/10.1016/j.renene.2016.04.083.

[8] D. Jin, M. Zhang, P. Wang, S. Xu, Energy 89 (2015) 178–190. https://doi.org/10.1016/j.energy.2015.07.069.

[9] A.S. Yadav, J.L. Bhagoria, Int. J. Therm. Sci. 79 (2014) 111–131. https://doi.org/10.1016/j.ijthermalsci.2014.01.008.

[10] K.R. Aharwal, B.K. Gandhi, J.S. Saini, Renewable Energy 33 (4) (2008) 585–596. https://doi.org/10.1016/j.renene.2007.03.023.

[11] M.M. Sahu, J.L. Bhagoria, Renewable Energy 30 (13) (2005) 2057–2073.

https://doi.org/10.1016/j.renene.2004.10.016.

[12] V.S. Hans, R.P. Saini, J.S. Saini, Sol. Energy 84 (6) (2010) 898–911. https://doi.org/10.1016/j.solener.2010.02.004.

[13] H.K. Ghritlahre, P.K. Sahu, S. Chand, Sol. Energy 199 (2020) 173–182. https://doi.org/10.1016/j.solener.2020.01.068.

[14] Y. Agrawal, J.L. Bhagoria, V.S. Pagey, Mater. Today Proc. 47 (2021) 6067–6073. https://doi.org/10.1016/j.matpr.2021.04.623.

[15] A.P. Singh, Varun, Siddhartha, Exp. Therm. Fluid Sci. 54 (2014) 117–126. https://doi.org/10.1016/j.expthermflusci.2014.02.004.

[16] R. Kumar, S.K. Verma, M. Singh, Mater. Today Proc. 44 (2021) 961–967. https://doi.org/10.1016/j.matpr.2020.11.006.

[17] Z. Jelonek, A. Drobniak, M. Mastalerz, I. Jelonek, Sci. Total Environ. (2020) 141267. https://doi.org/10.1016/j.energy.2022.125507.

[18] B. Bhushan, R. Singh, Sol. Energy 85 (5) (2011) 1109–1118. https://doi.org/10.1016/j.solener.2011.03.007.

SURESHKUMAR PETCHIMUTHU[1]

SATHIYA MOORTHY RAJENDRAN[2]

[1]Department of Mechanical Engineering, Government College of Engineering, Tirunelveli, India

[2]Department of Mechanical Engineering, Anna University Regional Campus, Coimbatore, India

NAUČNI RAD

EKSPERIMENTALNO PROUČAVANJE SOLARNOG GREJAČA VAZDUHA SA REBRIMA C OBLIKA OBLOŽENIM ZEOLITOM

U ovoj studija istraživane su brzina prenosa toplote i frikciona svojstva apsorbera sa solarnim grejačem vazduha sa C-rebrima, sa i bez perforacija, kao i efikasnost ovog apsorbera sa i bez zeolitne prevlake. Ovo istraživanje je sprovedeno u opsegu Rejnoldsovog broj (Re) od 3.000 do 18.000, sa C-rebrima, visine 2 mm i 4 mm, sa otvorom prečnika od 1 mm do 3 mm. Uticaj visine rebra, prečnika otvora i zeolitne prevlake na termičku efikasnost i Nuseltov broj se poredi sa ravnim kanalom pri istim protocima. Snažan sekundarni protok se stvara tako što se sloj slobodnog smicanja češće ponovno odvaja na većim visinama rebara, a manja rupa može uvećati prenos toplote i poboljšati efekat unakrsnog strujanja. Toplotna efikasnost i Nuseltov broj solarnog grejača vazduha sa C-rebrima (visina rebra = 4 mm i prečnik otvora = 1 mm) i zeolitnom prevlakom na apsorberu povećani su za 29,7% i 62,2% u odnosu na ravni apsorber. Rebra visine 4 mm mogu povećati trenje u kanalu do 3,1 puta u poređenju sa glatkim kanalom.

Ključne reči: C-rebra; perforacije; zeolitni prevlaka; toplotne performance; faktor trenja.